

CHAPTER 4: A DUAL BAND DUAL ANTENNA WITH READ RANGE ENHANCEMENT FOR UHF RFID TAGS

4.1 Introduction

As it is discussed in previous chapters, an UHF RFID system consists of two components viz., a reader and a tag. The reader transmits an interrogatory electromagnetic signal to the tag. A passive tag contains an antenna and a microchip. As the passive tag does not contain any internal power source, it receives power from the incoming signal. When the received power exceeds the minimum threshold power of the tag chip, the chip is activated and switches its input impedance between two different states according to stored data. In a conventional RFID tag, the microchip switches its load impedance between short-circuit state and complex conjugate to tag antenna state. The tag antenna works as a receiving antenna when the chip impedance is complex conjugate to it, and as a backscattering antenna when the chip impedance is short-circuited. For an impeccable tag design, there should be continuous power reception in order to keep the chip activated and to obtain longer read range, the difference in the level of backscattered field should be maximum [144]. Conventional tags have only one antenna, which serves as receiving as well as backscattering antenna, thereby giving rise to two crucial drawbacks. Firstly, the power reception by the tag chip would not be continuous when the chip impedance is switched to short-circuit state. As a result of this impedance mismatch between the chip and the tag antenna, the power absorption efficiency plunges considerably. Secondly, the level difference in backscattered signal would not be maximum due to the presence of two impedance states of the conventional microchip, namely the short circuit and the highly capacitive

state. To augment the shortcomings of conventional tags, dual tag antenna has been proposed. A dual antenna consists of two antennas; one is receiving antenna for continuous power absorption while the second one is backscattering antenna designed for the maximum level difference in backscattering signal. Each country has different frequency allocation for UHF RFID systems. Therefore, the design of RFID tags that are able to cover at least two of the regulated UHF bands is very promising for inter-country UHF RFID applications like import-export industry.

In this chapter, a single-sided dual band dual antenna has been proposed which operates at 866 MHz and 915 MHz UHF RFID bands. The presented structure is made up of two separate antennas. One antenna is entirely used for receiving and other is used for backscattering, thus, the necessity for maximum level difference in RCS and uninterrupted power supply to tag IC is fulfilled, simultaneously. The dual-band behaviour of receiving antenna is attained by adding a pair of thin slits on one radiating edge of the patch surface. The dual-band backscattering antenna is made up with a comb-shaped open ring and a meander line structure. Both the receiving and backscattering antennas have been designed on single side of the grounded substrate, thus enabling it be mounted on metallic objects without any performance deterioration. The performance of the proposed antenna is analysed in terms of RCS and read range on metallic objects and free space. All the simulations were carried out with finite element method based high frequency structure simulator (HFSS). The differential probe technique, which has been used to measure the differential impedance of the receiving and backscattering antennas, provides a good agreement between the simulated and measured results.

4.2 Dual Band Dual Antenna Concept and Design

4.2.1 Design Concept

Figure 4.1 depicts the schematics of the passive RFID tags. In a conventional RFID tag, an antenna of input impedance Z_a is connected with a tag IC of input impedance Z_L . The conventional tag IC switches its input impedance between two states, viz. matched (Z_{L1}) and short (Z_{L2}). In the match state, power is collected from the incoming signal and transferred to the tag IC and in the short state, the incoming signal is backscattered. The difference in the backscattered signals' strength (Δ) corresponding to the two impedance states (Z_{L1} and Z_{L2}) of the tag IC is proportional to

$$\Delta \propto |\Gamma(Z_{L1}) - \Gamma(Z_{L2})| \quad (4.1)$$

Where $\Gamma(Z_L)$ is a complex reflection coefficient and can be expressed as

$$\Gamma(Z_L) = \frac{Z_L - Z_a^*}{Z_L + Z_a} \quad (4.2)$$

The difference in the backscattered signal strength (Δ) should be maximum in order to maximize the read range of an RFID system. The maximum possible value of the quantity $|\Gamma(Z_{L1}) - \Gamma(Z_{L2})|$ could be 2, corresponding to two impedance loading states of $Z_{L1} = \infty$ and $Z_{L2} = 0$. $\Gamma(Z_{L1} = \infty) = 1$ and $\Gamma(Z_{L2} = 0) = -1$ when the antenna input impedance would be only real-valued. As shown in figure 4.1(a), conventional RFID tag employs only a single antenna for reception as well as backscattering purpose. Therefore, the impedance loading states for a maximum level difference in backscattering signal (Δ) would not be possible with simultaneous maximum power reception in conventional RFID tags.

A dual antenna consists of two antennas as shown in figure 4.1(b). One is receiving antenna, and other is backscattering antenna that provides maximum power reception with a maximum level difference in backscattered signal strength

simultaneously. In dual antenna tag structure, a modified three terminal tag IC is used instead of conventional two terminals IC. One terminal of the tag IC (R_{F1}) is connected with receiving antenna and the second terminal (R_{F2}) is connected with backscatter antenna and the remaining terminal is connected to the common ground of both the antennas.

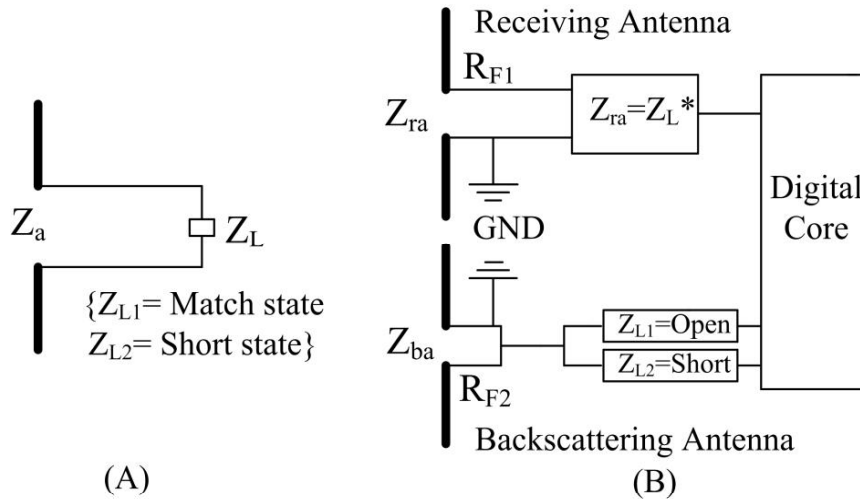


Figure 4.1 Schematic representation of passive RFID tags (A) Conventional (B) Dual antenna

4.2.2 Antenna Configuration

The designed dual band dual antenna configuration is shown in figure 4.2, and the optimized geometrical parameters are exhibited in Table 4.1. The proposed structure contains two independent dual-band antennas which are designed on an FR4 substrate of thickness 1.6mm with a relative permittivity 4.4 and loss tangent 0.02. The antenna is designed for NXP's UCODE 7 tag IC, which has an input impedance of $14.5-j293 \Omega$ and $12.5-j277 \Omega$ at 866 MHz and 915 MHz, respectively [12]. The input impedance of the receiving antenna should be complex conjugate to the chip impedance ($Z_{ra}=Z_L^*$) in order to maximize the power reception. Therefore, the imaginary part of the receiving antenna impedance has to be inductive at resonating frequencies. In the proposed

receiving antenna, an inset feed is used to provide required inductive impedance. By adjusting the length (L_4) and width (W_5) of inset feed, input impedance of antenna can be controlled. The dual-band behaviour of receiving antenna is realized by etching a pair of thin slits of width (W_6) and length (L_2) on one radiating edge of the inset feed microstrip antenna. The pair of thin slits on the radiating edge of the antenna excites a new resonant mode with surface current length of 0.53 times the guided wavelength at 915 MHz frequency due to the disturbance of surface current distribution [83], [168]. Though the receiving antenna has two resonant frequencies, its size seems to be too large. Therefore, three pairs of nonuniform length (L_5, L_6, L_7) slits are embedded on the nonradiating edges to reduce antenna size [169].

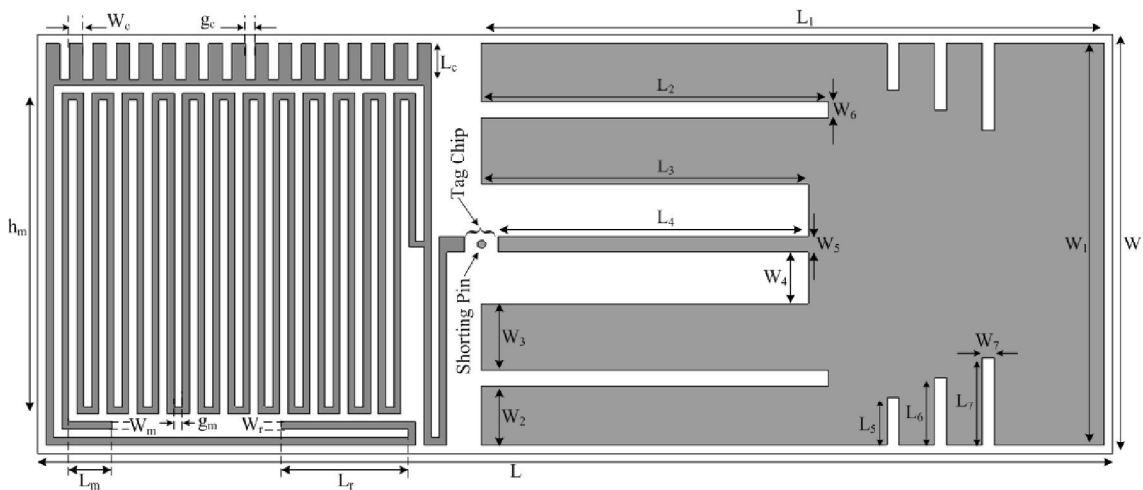


Figure 4.2 Configuration of the dual-band dual antenna structure

The dual-band backscattering antenna consists of two sections; an open ring element and a meander line structure. The meander line structure is excited within the open ring element. Uniform length horizontal elements of size $L_c \times W_c$ are added to the open ring monopole antenna to disperse the current distribution and the capacitance of antenna is increased [170], [171]. The current path in the open ring structure is also increased by comb-shaped horizontal elements, therefore, the higher resonant frequency (f_2) will be decreased. For the fine-tuning of resonant frequency f_2 , a tuning stub of

length L_r is extended at the end of open ring element. The resonant frequency f_1 is excited by extending a meander line structure inside the open ring element to keep the size of antenna unchanged. The tuning of resonant frequency f_1 is achieved by tuning the gap (g_m) and width of the meander line (W_m). For further tuning, a stub of length L_m is extended at the end of meander structure.

Table 4.1 Optimized geometrical parameters of the dual-band dual antenna

Parameter	Value (mm)	Parameter	Value (mm)
L	128.3	W	50
L_1	74.3	W_1	48
L_2	41.4	W_2	7
L_3	39	W_3	8
L_4	37	W_4	6.1
L_5	5.7	W_5	2
L_6	8	W_6	1.9
L_7	10.4	W_7	1.4
L_c	4.3	W_c	1.6
L_r	15.1	W_r	0.9
L_m	5.2	W_m	0.8
g_c	1.2	g_m	1
h_m	38.3		

4.3 Results and Discussions

The fabricated prototype of the proposed dual-band dual antenna with a differential probe is shown in figure 4.3. For experimental verification, all the measurements are carried out with Anritsu MS2038C VNA. The S-parameter measurements of receiving and backscattering antennas are performed using port extension technique with a differential probe. The differential impedance of the receiving and the backscattering antennas are obtained from measured S-parameters. This section discusses about the various results obtained during the analysis of the designed antenna structure. The results which are discussed in the following subsections

include the performance of receiving and backscattering antenna in terms of input impedance characteristics, reflection coefficient characteristics, radiation patterns and isolation. Detection range of the dual antenna is also compared with the conventional antenna at both operating frequency bands.

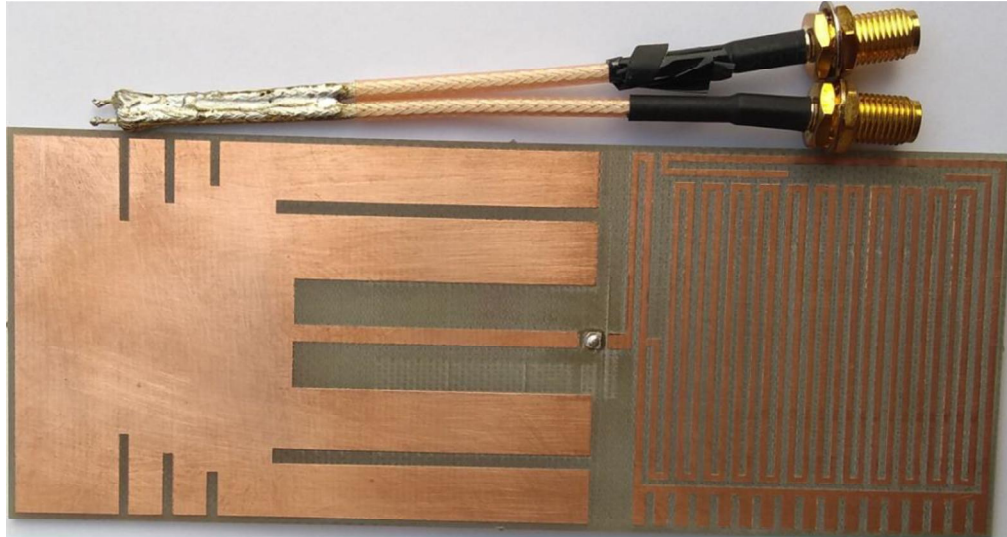


Figure 4.3 Fabricated prototype of the dual band dual antenna with a differential probe

4.3.1 Performance of Receiving Antenna

The simulated and measured input impedance of the receiving antenna are shown in figure 4.4. The conjugate input impedance of NXP's UCODE 7 microchip at different frequencies is also plotted. The input impedance plot indicates that the resistance and reactance values of the receiving antenna are varied around the complex conjugate impedance of the microchip at both 866 MHz and 915 MHz frequencies. The simulated and measured input impedances at 866 MHz (915 MHz) are calculated as $14+j293.85 \Omega$ ($14.13+j276.58 \Omega$) and $15.51+j294.45 \Omega$ ($11.7+j275.96 \Omega$), respectively, which are fairly close to the complex conjugate of chip impedance. The power reflection coefficient of the receiving antenna is calculated from the input impedance results by using equation 4.2. Figure 4.5 shows the simulated and measured reflection coefficient of the receiving antenna with frequency. The result illustrate that the simulated 10 dB

return loss bandwidth of the receiving antenna is 9 MHz (863-872 MHz), and 11 MHz (911-922 MHz) and corresponding measured 10 dB return loss bandwidth is 10 MHz (863-873 MHz) and 12 MHz (913-925 MHz), which covers the UHF RFID band of North America and Europe. Good agreement between the simulated and measured results is found at both frequency bands.

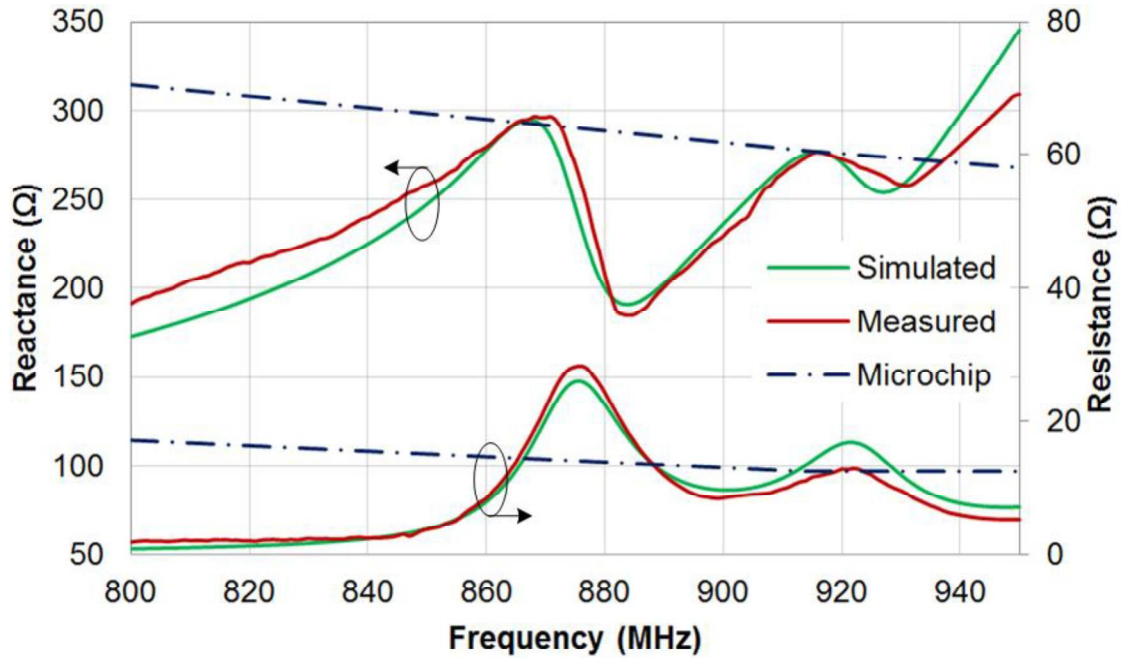


Figure 4.4 Simulated and measured input impedance of the receiving antenna

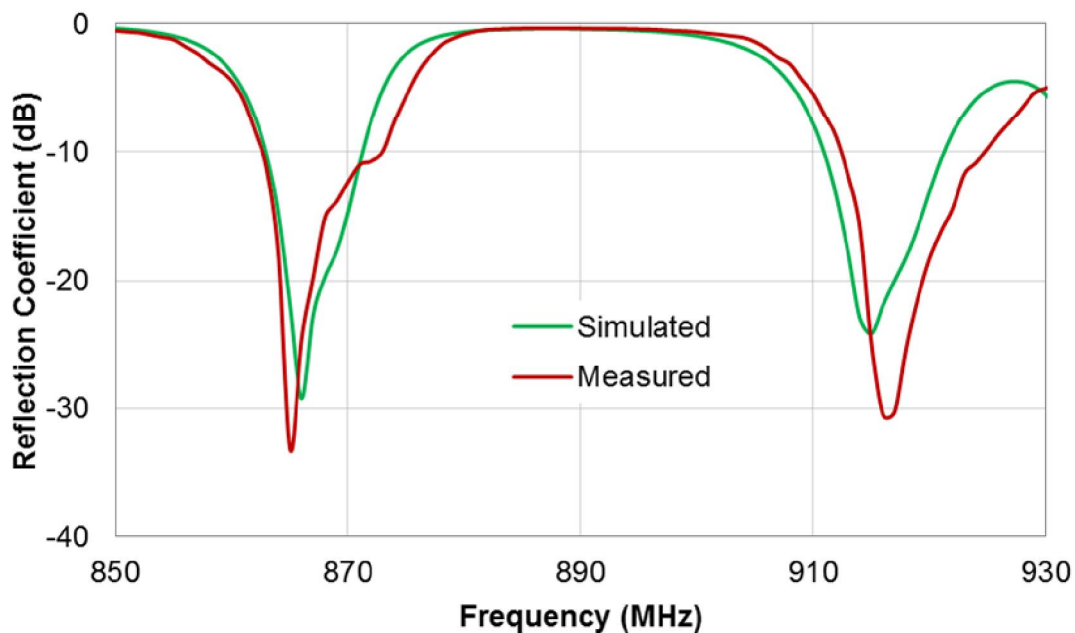


Figure 4.5 Simulated and measured reflection coefficient against frequency for the receiving antenna

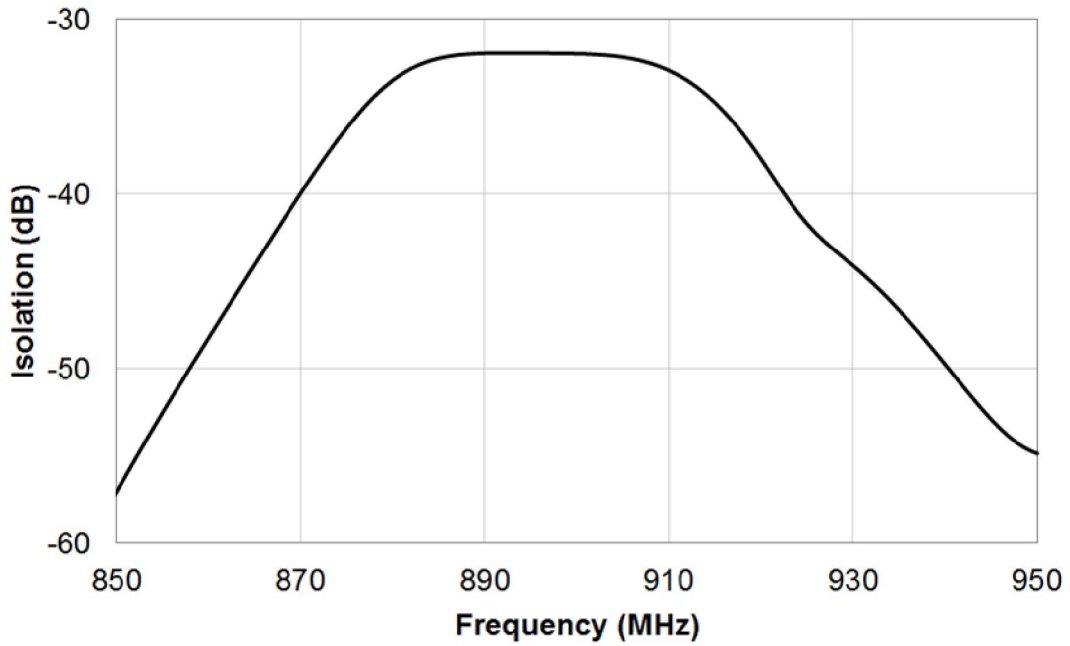


Figure 4.6 Isolation between receiving and backscattering antenna

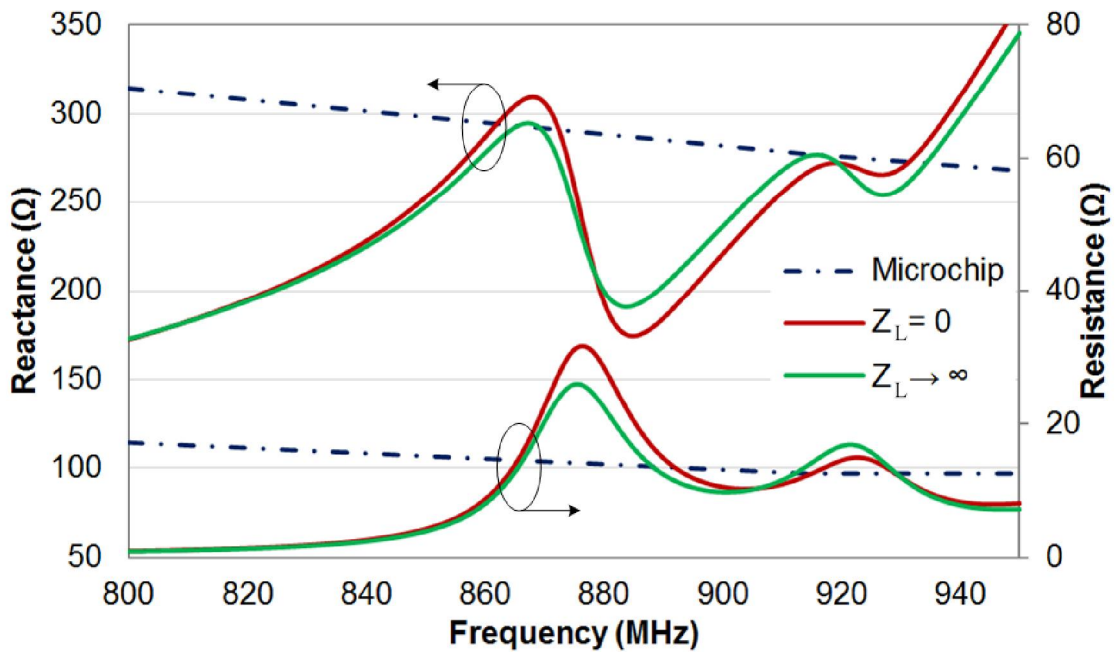


Figure 4.7 Input impedance of the receiving antenna with backscattering antenna being short circuit ($Z_L=0$) and open circuit ($Z_L=\infty$)

The simulated isolation response of the designed dual antenna geometry is displayed in figure 4.6. At 866 MHz and 915 MHz, the isolation levels of the designed antenna are -43.2 dB and -34.75 dB, respectively, which illustrates the low mutual coupling between the receiving antenna and the backscattering antenna. Due to the low

mutual coupling, the input impedance of the receiving antenna remains nearly unaltered with the short circuit and open circuit impedance loading of the backscattering antenna. The simulated input impedance of the receiving antenna when backscattering antenna is terminated with open ($Z_L=\infty$) and short ($Z_L=0$), is exhibited in figure 4.7. At 866 and 915 MHz, the input impedance of the receiving antenna when the backscattering antenna is terminated as short-circuited (open circuited) are $15.24+j307.03 \ \Omega$ ($14+j293.85 \ \Omega$) and $12.52+j268.27 \ \Omega$ ($14.13+j276.59 \ \Omega$), respectively. The low variation in input impedance of the receiving antenna with different loading of backscattering antenna demonstrates that the power reception by the receiving antenna would remain uninterrupted during the backscattering modulation.

A conventional single antenna tag structure is also optimised for the comparison purpose in which only a single antenna works as receiving antenna as well as backscattering antenna. The simulated radiation pattern of the conventional antenna and proposed dual antenna at 866 MHz and 915 MHz are presented in figure 4.8 and figure 4.9, respectively. The radiation pattern for the designed dual antenna structure is plotted for two cases with its backscattering antenna open-circuited and short-circuited. The E-plane and H-plane radiation pattern of the proposed dual antenna in both cases remain identical to the conventional antenna.

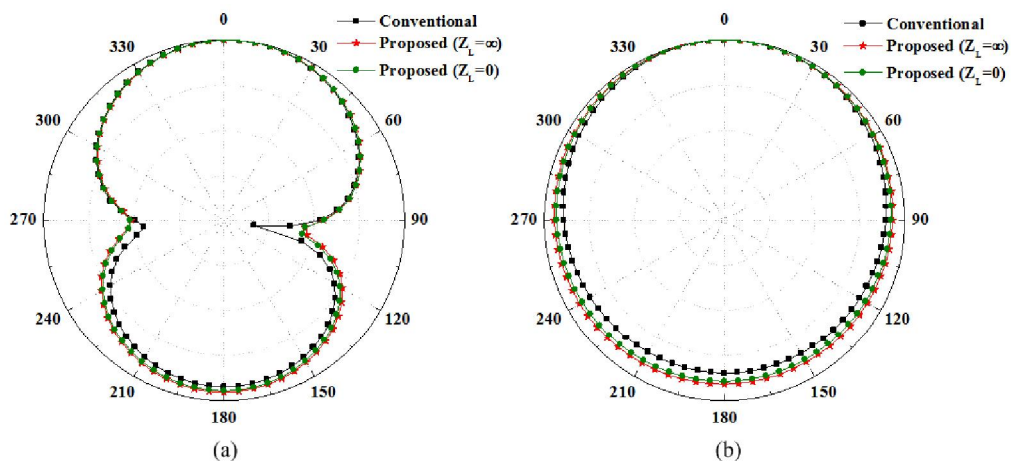


Figure 4.8 Radiation patterns of the dual antenna at 866 MHz (a) XZ plane, (b) YZ plane

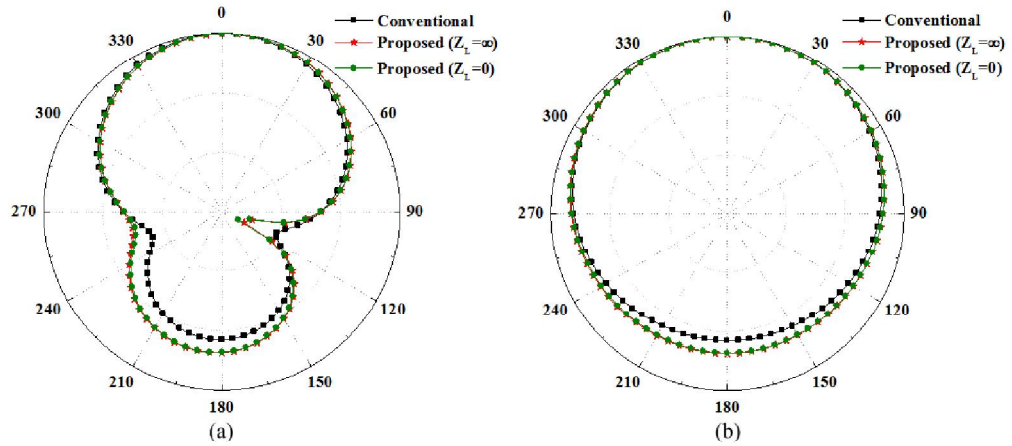


Figure 4.9 Radiation patterns of the dual antenna at 915 MHz (a) XZ plane, (b) YZ plane

4.3.2 Performance of Backscattering Antenna

The simulated and measured input impedances of the backscattering antenna are shown in figure 4.10. The simulated and measured input impedances at 866 MHz are $141.09-j1.98 \Omega$ and $117.9+j0.62 \Omega$ and at 915 MHz are $30.38+j0.59 \Omega$ and $28.98-j2.89 \Omega$, respectively. At both the resonating frequencies, the reactance values of input impedance are close to zero, which is requisite for the maximum level difference of the backscattering signal.

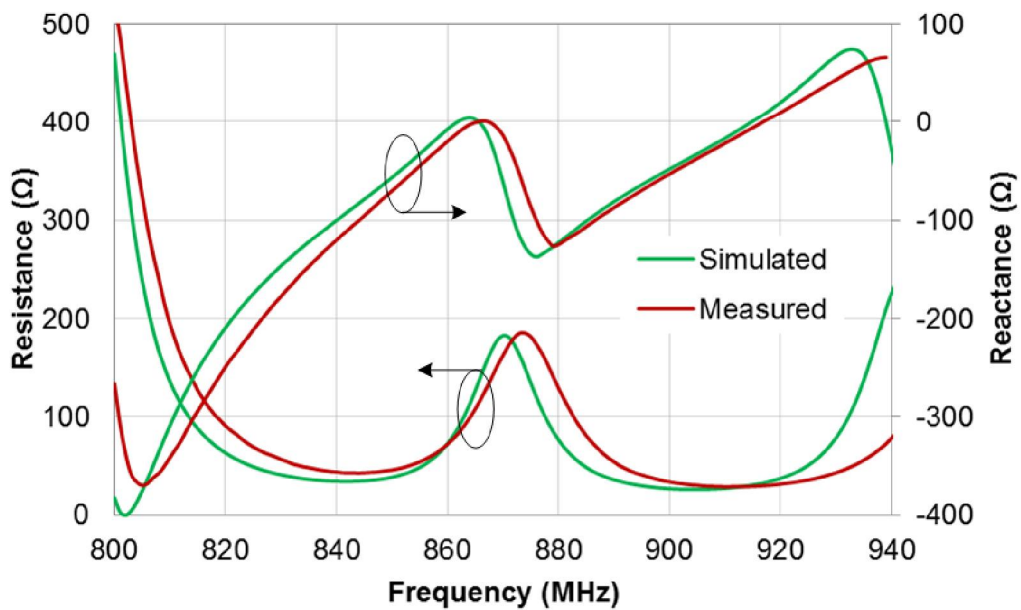


Figure 4.10 Simulated and measured input impedance variation of the backscattering antenna

For the polarisation-matched reader and tag antennas, the backscattered radar cross section (σ) of the tag antenna is calculated by using equation (2.7). RCS of the proposed dual antenna for the two loading states (short-circuit; $Z_L=0$ and open-circuit; $Z_L=\infty$) and the RCS of the conventional single antenna for the two loading states (short-circuit; $Z_L=0$ and match-state; $Z_L=Z_C$) are plotted in figure 4.11 and figure 4.12, respectively. RCSs of the conventional and dual antennas at 866 MHz and 915 MHz are summarised in table 4.2. The differential RCS ($\Delta\sigma$) for the two loading states of the proposed dual antenna is 44.60 dBsm and 45.13 dBsm at 866 MHz and 915 MHz, respectively. For the conventional single antenna, the differential RCS ($\Delta\sigma$) are 2.73 dBsm and 2.67 dBsm at 866 MHz and 915 MHz, respectively. It is observed from table 4.2 that in case of the proposed dual antenna, the differential RCS ($\Delta\sigma$) is raised from 2.73 dBsm to 44.60 dBsm at 866 MHz and from 2.67 dBsm to 45.13 dBsm at 915 MHz. This augmentation in differential RCS in case of dual-antenna enhances the read range.

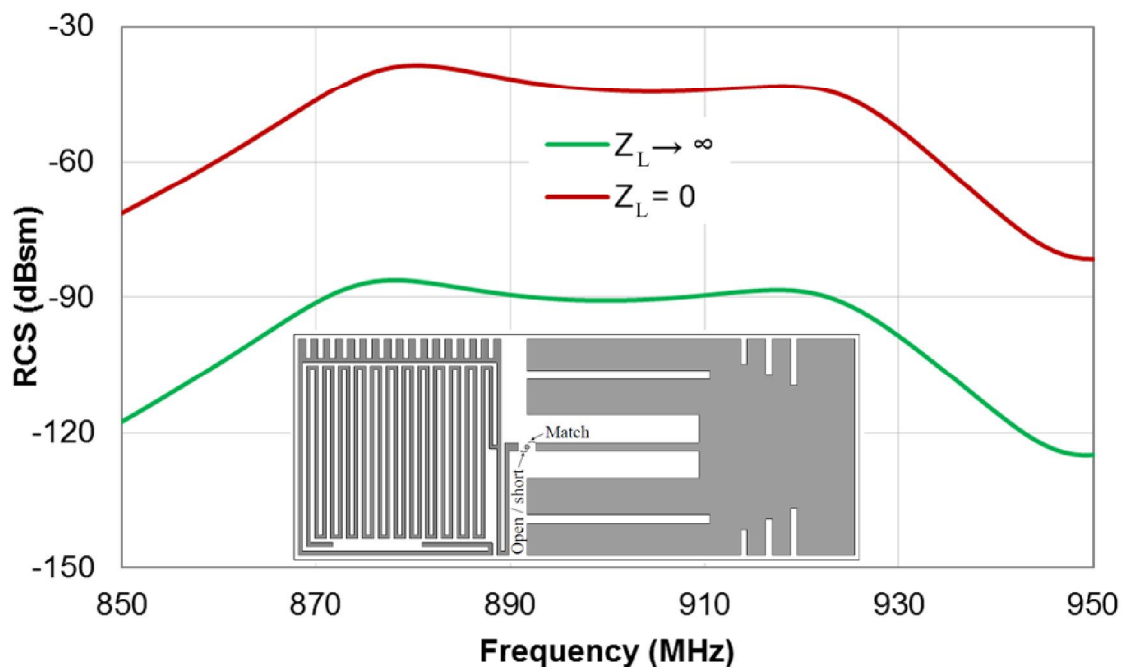


Figure 4.11 Backscattering RCS of the dual antenna when the receiving antenna is conjugately matched and backscattering antenna in two states (open and short)

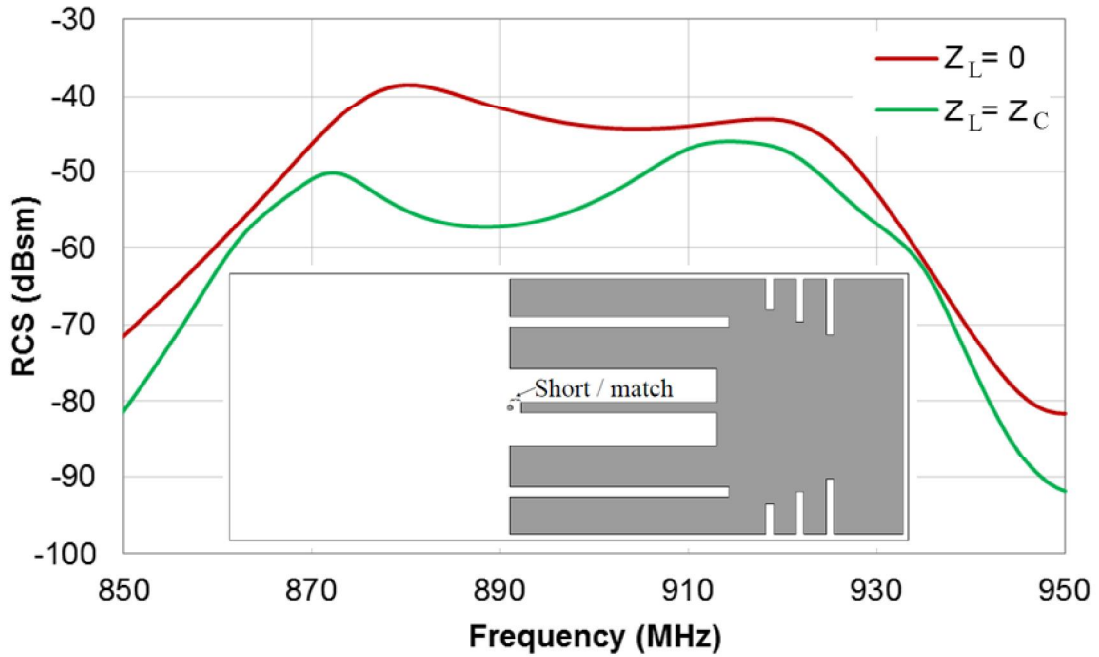


Figure 4.12 Backscattering RCS of conventional single antenna when in two states (match and short)

Table 4.2 Backscattering RCS of conventional and dual antennas at 866 MHz and 915 MHz

Operating Frequency (MHz)	RCS (dBsm)	Conventional Antenna	Proposed Dual-antenna
866	Maximum	-51.73	-51.73
	Minimum	-54.46	-96.34
915	Maximum	-43.42	-43.42
	Minimum	-46.09	-88.55

The maximum read range (R_{\max}) between the reader and the tag can be evaluated by classical radar range equation (2.6). The maximum read ranges of the designed dual antenna and the conventional antenna are plotted in figure 4.13. For RFID systems, the effective isotropic radiated power (EIRP) is regulated as 3.3 W and 4 W in Europe and North America, respectively [19]. Due to the proposed dual-antenna, the maximum read range is enhanced from 3.5 m to 4.3 m at 866 MHz and from 5.6 m to 6.8 m at 915 MHz.

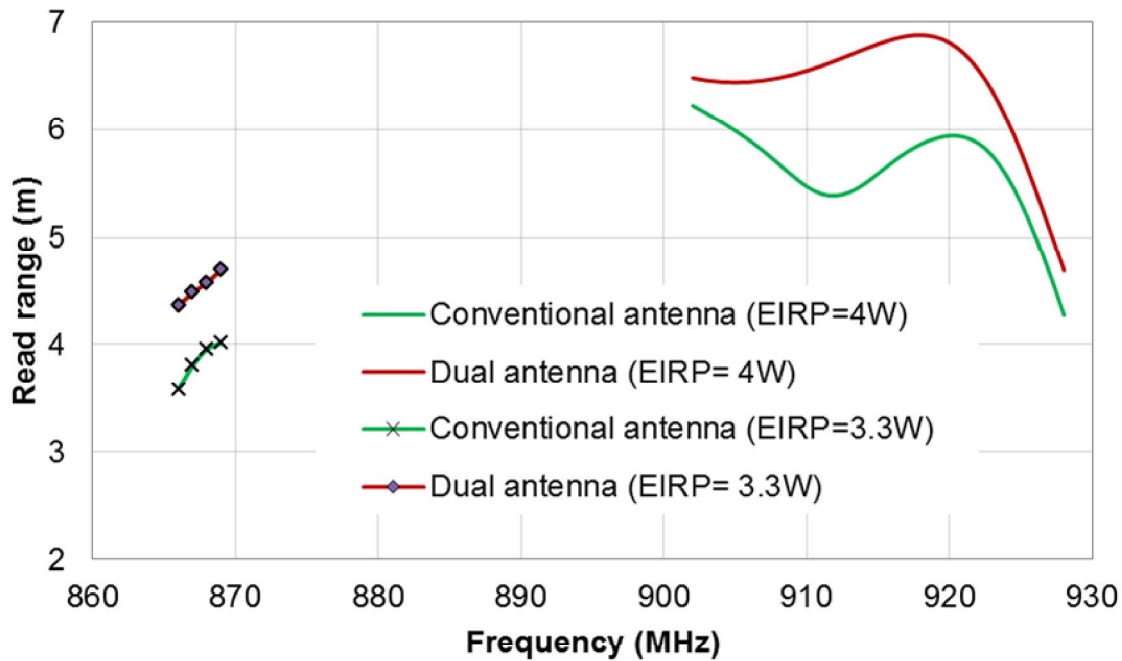


Figure 4.13 Detection range comparison of the dual antenna and conventional antenna

4.4 Performance of the Dual Antenna on Metallic Surface

There is only one normal component of the electric field and tangential component of the magnetic field on a perfect electric conductor. Thus, the dipole type RFID tag antennas whose performance relies on a tangential component of the electric field may suffer from severe performance degradation when it is mounted on the conductive surface [20]. Performance of the designed dual antenna in terms of the input impedance and maximum read range is examined when it is attached to the different size of metallic platforms. Figure 4.14 illustrates the simulated input resistance and reactance values of the receiving antenna with a different size of metallic surface. The input impedance variation with and without different metallic surfaces is small, which shows that the receiving performance of the proposed antenna remains unchanged. The gain of the proposed dual antenna is enhanced when it is mounted on the metallic surface than the air because of the reflection effect of the metal. A smaller size metallic sheet ($128 \times 50 \text{ mm}^2$) attains a lower gain compared to a larger metallic sheet ($250 \times$

100 mm²). Comparable gain is observed when the metallic surface size is further increased to 250 × 100 mm². Due to gain enhancement, the read range of the proposed dual antenna is also increased when it is mounted on the metallic objects. Table 4.3 shows the maximum read range for the designed dual antenna with different sizes of metallic sheet.

Table 4.3 Maximum read range of the proposed dual antenna attached to different size metallic objects

Measurement Condition	Simulated Maximum Gain G_t (dB)		Maximum Read Range (m)	
	866 MHz	915 MHz	866 MHz (EIRP=3.3 W)	915 MHz (EIRP=4.4 W)
Without Metallic Sheet	-12.56	-4.98	4.3	6.8
128×50 mm ² Metallic Sheet	-8.7	-1.83	5.1	7.8
250×100 mm ² Metallic Sheet	-7.4	-1.09	5.5	8.2

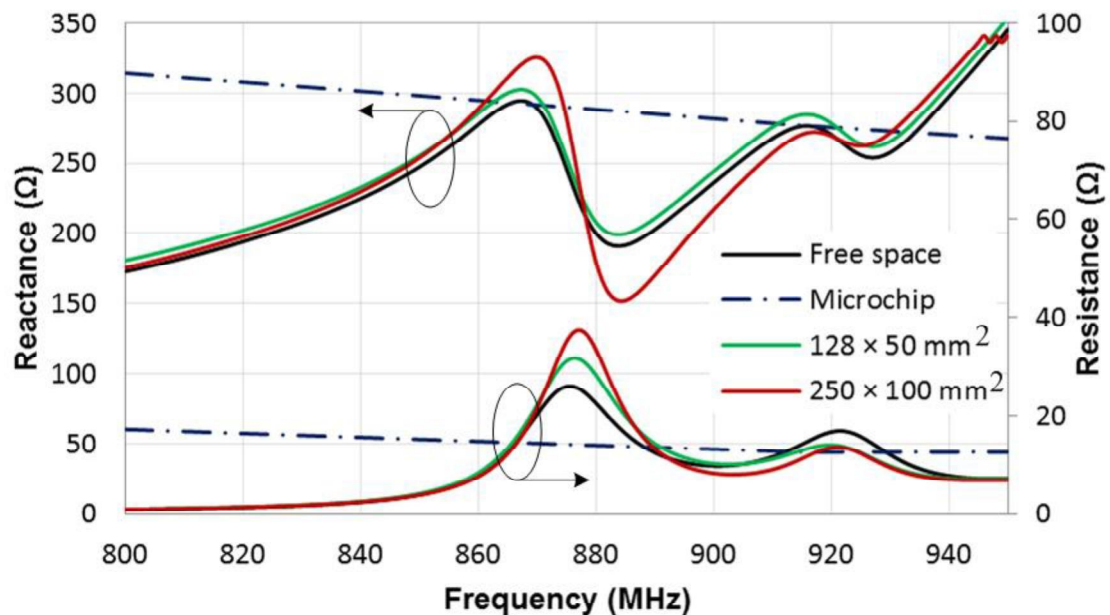


Figure 4.14 Simulated input impedance of the receiving antenna with different size of metallic surfaces

4.5 Conclusion

In this chapter, a dual band dual antenna for 866 MHz and 915 MHz UHF RFID tag applications has been presented. The designed antenna consists of two antennas; one is the receiving antenna, and other is the backscattering antenna. For continuous maximum power reception, the receiving antenna has input impedance complex conjugate to the input impedance of tag IC. The backscattered antenna is designed to have only real input impedance for the maximum differential RCS which results in read range enhancement. The differential RCS and maximum read range of the proposed dual antenna are 44.60 dBsm and 4.3 m at 866 MHz and 45.13 dBsm and 6.8 m at 915 MHz. Due to the low mutual coupling between the receiving and the backscattering antennas, the performance of the receiving antenna is not affected by the two loading states (short and open) of the backscattering antenna. The proposed dual antenna has a good performance on metallic sheets in both European and North American bands.

Circularly polarized antennas with directional radiation pattern are preferred for RFID reader as it can detect a linearly polarized tag irrespective of the orientation. CP reader antenna also increases polarisation efficiency in case of circularly polarised tag antenna. By keeping above facts in mind, a single feed circularly polarised antenna for handheld UHF RFID reader is presented in the next chapter.